

Increased Dispersion of Supported Gold during Methanol Carbonylation Conditions

Alexandre Goguet,[†] Christopher Hardacre,^{*,†} Ian Harvey,[‡] Katabathini Narasimharao,[†] Youssef Saih,[†] and Jacinto Sa[†]

CentACat, School of Chemistry and Chemical Engineering, Queen's University, Belfast, BT9 5AG, U.K., and Synchrotron Radiation Source, Daresbury Laboratory, Warrington, Cheshire, WA4 4AD, U.K.

Received March 25, 2009; E-mail: c.hardacre@qub.ac.uk

Both transition and platinum group metal homogeneous and heterogeneous catalyzed carbonylation of methanol have been well documented.^{1–5} Although the efficiency of the homogeneous process has been clearly demonstrated, heterogeneous catalysts offer the advantages of facile product separation and vapor phase operation which limit the loss of catalyst.

Recently, Zoeller et al. reported that gold supported on carbon has been found to be very active and selective for the reaction of carbonylation of methanol to methyl acetate.⁶ Therein, a 1% Au/C catalyst was demonstrated to be as least as active as its iridium counterpart, previously regarded as the most active and selective catalytic material. However, the high activity of the gold catalyst is only achieved after an induction period of several hours. To date, there is no understanding regarding the origin of this induction period. Herein, the evolution of the structure of two supported gold catalysts during the carbonylation of methanol in the presence of methyl iodide has been examined to correlate it with their on stream activity. Of particular importance for this reaction is the role of methyl iodide in modifying the catalyst active site. The understanding of gold based catalysts is of significant current interest for both this particular reaction and more generally.^{7–10} Two 1 wt % Au supported on activated carbon catalysts were supplied by the World Gold Council and Eastman Chemicals. Throughout the paper, the catalysts are denoted Au^{WGC}/C and Au^{Eastman}/C, respectively, with the latter being that used in the commercial process.

Figure 1 shows a comparison of the rate of production of methyl acetate as a function of time on stream over the Au^{WGC}/C and Au^{Eastman}/C catalysts. While the Au^{WGC}/C catalyst shows high initial activity producing $\sim 8 \text{ mol h}^{-1} \text{ g}_{\text{Au}}^{-1}$, much lower initial activity is observed for the Au^{Eastman}/C catalyst. As the reaction proceeds, a gradual increase in activity was found for the Au^{WGC}/C reaching 9–10 $\text{mol h}^{-1} \text{ g}_{\text{Au}}^{-1}$ after 80 h of reaction. In contrast, a much larger increase in activity occurs for the Au^{Eastman}/C catalyst with both catalysts reaching the same activity after 80 h of reaction. The general trend in activity for this catalyst under our conditions is similar to that reported by Zoeller et al., although therein, little activity was observed over the first 20 h on stream.

For both catalysts, XRD shows large gold particles of 12 and 28 nm diameter for the Au^{WGC}/C and Au^{Eastman}/C catalysts, respectively (Figure 2). No other peaks apart from those associated with the carbon support were observed. A major transformation is found after reaction with the resultant diffraction pattern showing only very small peaks associated with residual gold metal. The TEM results are in agreement with the average gold particle sizes of both fresh catalysts, derived from XRD analysis (Figure 3a and b). TEM results for both spent Au^{WGC}/C and Au^{Eastman}/C catalysts did not

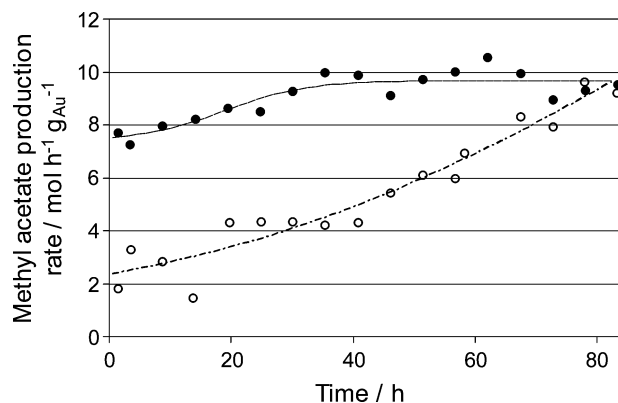


Figure 1. Comparison of rate of formation of methyl acetate as a function of time on stream for the Au^{WGC}/C (●) and Au^{Eastman}/C (□) catalysts.

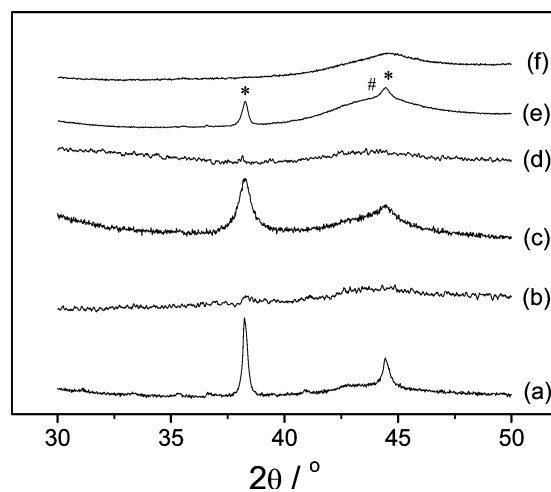


Figure 2. Ex-situ XRD patterns of fresh (a) Au^{Eastman}/C and (c) Au^{WGC}/C catalysts and (b) Au^{Eastman}/C and (d) Au^{WGC}/C catalysts following 80 h reaction at 16 bar and 240 °C. Diffractograms (e) and (f) show the Au^{WGC}/C catalyst after 5 and 15 min exposure to 0.034% methyl iodide in N₂ at atmospheric pressure and 240 °C, respectively. “*” denotes the diffraction features associated with metallic gold and “#” denotes carbon.

show any observable gold particles (Figures 3c and d). Furthermore, elemental analysis showed no significant difference in the gold loading between fresh and spent catalysts.

The Fourier transforms for the fresh Au^{Eastman}/C catalyst following EXAFS analysis, during and after reaction, are shown in Figure 4 with the interatomic distances and coordination numbers used to fit the EXAFS data for both catalysts shown in Table 1. In agreement with the XRD and TEM, the EXAFS of the fresh catalysts shows large gold particles. For the Au^{WGC}/C catalyst, after

[†] Queen's University.
[‡] Daresbury Laboratory.

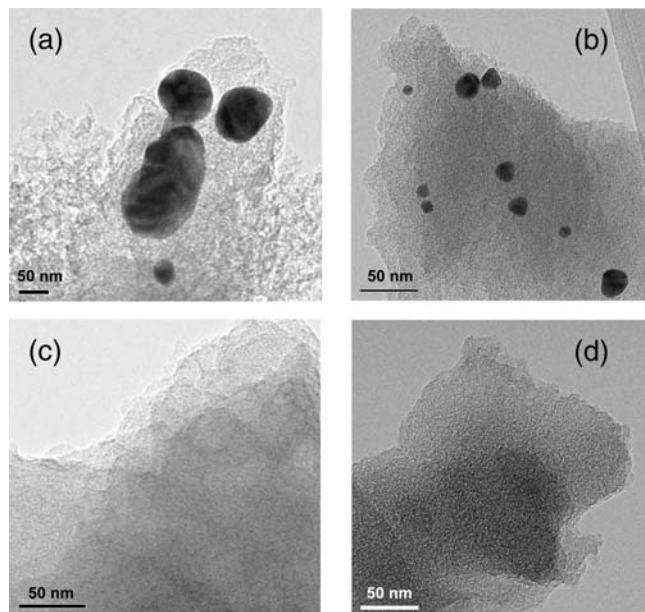


Figure 3. TEM pictures of (a) fresh Au^{Eastman}/C, (b) fresh Au^{WGC}/C, (c) Au^{Eastman}/C following reaction, and (d) spent Au^{WGC}/C following reaction.

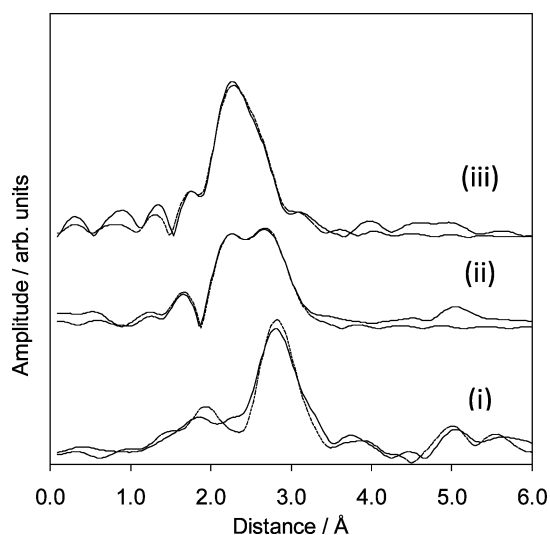


Figure 4. Comparison of the experimental (solid line) and fitted (dashed line) Fourier transforms from the Au L_{III} EXAFS data of Au^{Eastman}/C catalyst (i) fresh and following (ii) 10 h and (iii) 80 h reaction.

2.5 h of reaction, the EXAFS changes dramatically with a peak in the Fourier transform appearing at 2.54 Å and a large decrease in the amplitude of the peak at 2.85 Å associated with Au...Au coordination. In addition, the peaks >3.5 Å associated with higher order coordination shells of gold disappear. This clearly indicated Au particles restructuring leading to extensive redispersion of the gold particles. The additional peak observed at 2.54 Å may be fitted to a Au...I distance and is consistent with bond lengths found in bulk AuI.¹¹ No significant change in the EXAFS is observed during reaction, thereafter. Similar changes are also observed for the Au^{Eastman}/C catalyst; however, in this case the transformation is much more gradual. Even after 10 h on stream, only partial redispersion had occurred as shown by the decrease in Au...Au coordination from 12.0 to 3.1. Following 80 h of reaction, the Au^{Eastman}/C catalyst had a Au...Au and a Au...I coordination number of ~1, i.e., similar to that found for the Au^{WGC}/C catalyst throughout the reaction,

Table 1. Structural Parameters from the Fitted Au L_{III} Edge EXAFS Spectra for the WGC and Eastman Catalysts as Received and during Reaction

catalyst	reaction time/h	atom ^a	distance/Å	coordination number	
Au ^{WGC} /C	0	Au	2.85	12.0	
		Au	4.06	6.0	
	2.5	I	2.54	1.5	
		Au	2.85	1.2	
		I	2.54	0.9	
		Au	2.85	0.9	
Au ^{Eastman} /C	0	Au	2.86	12.0	
		Au	4.06	6.0	
	10	I	2.54	1.3	
		Au	2.86	3.1	
		80	I	2.55	1.0
			Au	2.87	1.0

^a First two shells shown for clarity.

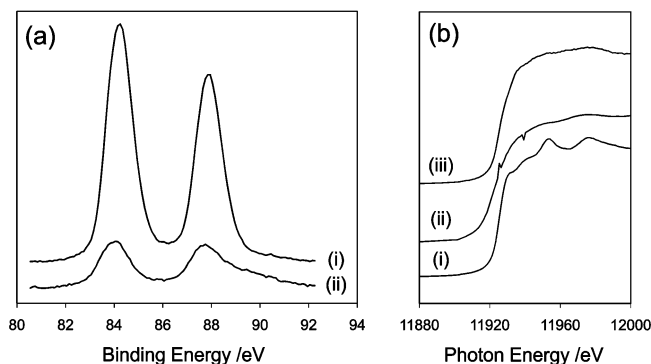


Figure 5. Comparison of the (a) Au 4f photoelectron spectra of the Au^{WGC}/C catalyst (i) as received and (ii) after 80 h reaction and (b) Au L_{III} XANES of the Au^{WGC}/C catalyst (i) as received, (ii) after 2.5 h reaction, and (iii) after 80 h reaction.

suggesting that the rate of dispersion may be related to the initial gold particle size. Using the XRD and TEM to estimate the particle size, the gold surface area is ~2.3 times higher for the Au^{WGC}/C catalyst compared with that for Au^{Eastman}/C, assuming the same particle shape in each case. The high initial activity observed for the Au^{WGC}/C (Figure 1) may be related to the fact that the catalysts were exposed for 1 h to the feed before the gas chromatographic analysis was started and may have resulted in a significant redispersion of the gold prior to the first activity measurement. This interpretation is supported by the XAS data (Table 1) which shows that 2.5 h of exposure to the reaction conditions led to significant gold redispersion. Further support is provided by the fact that an independent XRD investigation of the behavior of the Au^{WGC}/C under 0.034% methyl iodide in nitrogen at atmospheric pressure and 240 °C showed a complete loss in gold features within 15 min of exposure (Figure 2).

In the case of the Au^{Eastman}/C, although this catalyst was also exposed for 1 h to the feed prior to the gas chromatographic analysis, the rate of gold redispersion is clearly slower as evidenced by the XAS data showing that 10 h were necessary to reach the similar extent of redispersion observed with the Au^{WGC}/C after only 2.5 h of exposure (Table 1). This difference in the rate of redispersion of the gold between the catalysts is in line with the smaller exposed gold surface area as a result of the larger particle size for the Au^{Eastman}/C catalyst compared with the Au^{WGC}/C material.

The oxidation state of the gold has been examined using XANES and XPS measurements (Figure 5). No significant change in the XANES white line intensity was found for either catalyst as a

function of the reaction time with the spectra representative of Au⁰⁺.¹² Similarly, the Au 4f_{7/2} peaks show little change over the course of the reaction except for a decrease in peak intensity due to shielding from the iodine. For each catalyst, binding energies of 84.0–84.2 eV were found. This may be compared with the binding energies of ~84.0 eV reported for bulk Au metal¹³ and 84.4 eV for AuI.¹⁴

The structural and electronic data coupled with the steady state activity are consistent with the catalyst transforming from large bulk gold particles to small clusters of gold containing 2–3 atoms stabilized by iodide, for example (Au₂I)⁰⁺ or (Au₃I)⁰⁺. It should be noted that the small changes in XANES and XPS observed despite the formal change between Au⁰ and an oxidized form is due to the weak ionic nature of the Au–I bond. This is consistent with the small shift in the XPS from bulk Au to AuI.^{13,14} As the average coordination number of the gold decreases, the activity of the catalyst increases for the carbonylation which may be related to the ability of the gold to adsorb and dissociate H₂ and adsorb CO.

Redispersion has been observed for supported Pt, Rh, Pd, and Ag catalysts following high temperature oxidation and reduction treatments;^{15–22} for example oxychlorination has been reported extensively as a method of redispersing Pt catalysts. However, such a change from bulk metal to near-atomically dispersed metal in the case of supported Au catalysts has not been reported previously. Increased dispersion of gold on the adsorption of CO at 300 °C on Au/CeO₂ has recently been reported by Romero-Sarria et al.²² Therein, the extent of redispersion was limited as evidenced by the presence of gold in the XRD, indicative of metal particles of 4 nm or above, after CO treatment. In the present study near atomic redispersion of the gold from particles >10 nm was achieved.

The activity and stability of the catalysts examined in the present study are even more striking, since it is commonly assumed that halide remaining after the catalyst preparation can have a large negative effect on the activity of gold based heterogeneous catalysts. For example, Au/CeO₂ utilized for CO oxidation shows reduced activity if chloride was not removed effectively from the catalyst during preparation.²³ Interestingly, an XRD investigation of Au^{WGC}/C under 0.034% methyl chloride in nitrogen at atmospheric pressure and 240 °C did not show a decrease in the gold features. In fact a slight narrowing of the peaks was observed indicating an increase in average particle size and is in clear contrast with the behavior of this catalyst in the presence of methyl iodide. This may be associated with the lower strength of the H₃C–I bond compared with the H₃C–Cl and shows the peculiar role played by iodine in these systems. Furthermore, this shows the unexpected behavior of gold compared with other metals where alkyl chlorides do result in increased dispersion, for example in the case of platinum.¹⁸

In summary, in the present study the active site in heterogeneous gold based catalysts for the carbonylation of methanol has been identified as dimers/trimers of gold with the iodide being critical for the activation of the catalyst and to maintain the catalyst in the active form. In a wider context, this study shows that it may be possible to reactivate gold catalysts after reaction. Although many gold based catalytic systems show high activity and selectivity for

a wide range of redox processes, for example,^{8,24,25} their practical application is often limited due to low stability. Irreversible deactivation has been shown to be associated with sintering of gold⁹ or loss of metal–support interaction,^{10,26} and, therefore, if it were possible to redisperse the metal, this would be of significant benefit in reactivating gold based catalysts. The present study demonstrates that the use of methyl iodide based thermal treatments may allow achieving such redispersion. Moreover, preliminary diffuse reflectance UV spectroscopy studies indicated that similar results are also obtained for gold catalysts supported on a range of metal oxides (ZrO₂, Al₂O₃, and TiO₂).

Acknowledgment. The authors gratefully acknowledge EPSRC for funding under the CASTech grant.

Supporting Information Available: Catalysts description, catalytic tests conditions, X-ray absorption spectra, and parameters values characterizing the catalysts at different reaction times. This information is available free of charge via the Internet at <http://pubs.acs.org/>.

References

- (1) Howard, M. J.; Jones, M. D.; Roberts, M. S.; Taylor, S. A. *Catal. Today* **1993**, *18*, 325.
- (2) Maneck, H.-E.; Gutschick, D.; Burkhardt, I.; Luecke, B.; Miessner, H.; Wolf, U. *Catal. Today* **1988**, *3*, 421.
- (3) Gelin, P.; Naccache, C.; Bentaarit, V. *Pure Appl. Chem.* **1988**, *60*, 1315.
- (4) Fujimoto, K.; Bischoff, S.; Omata, K.; Yagita, H. *J. Catal.* **1992**, *133*, 370.
- (5) Liu, T. C.; Chiu, S. J. *Ind. Eng. Chem. Res.* **1994**, *33*, 488.
- (6) Zoeller, J. R.; Singleton, A. H.; Tustin, G. C.; Carver, D. L. U.S. Patent No. 6,506,933 and No. 6,509,293.
- (7) For example Haruta, M.; Kobayashi, T.; Sano, H.; Yamada, N. *Chem. Lett.* **1987**, *2*, 405.
- (8) Hashmi, A. S. K.; Hutchings, G. J. *Angew. Chem., Int. Ed.* **2006**, *45*, 7896.
- (9) For example Fu, Q.; Salzburg, H.; Flytzani-Stephanopoulos, M. *Science* **2003**, *301*, 935.
- (10) Tibiletti, D.; AmieiroFonseca, A.; Burch, R.; Chen, Y.; Fisher, J.; Goguet, A.; Hardacre, C.; Hu, P.; Thompson, D. *J. Phys. Chem. B* **2005**, *109*, 22553.
- (11) Jagodzinski, H. Z. *Kristallogr., Kristallphys., Kristallchem.* **1959**, *112*, 80.
- (12) Choy, J. H.; Kim, Y. I. *J. Phys. Chem. B* **2003**, *107*, 3348.
- (13) Wagner, C. D.; Naumkin, A. V.; Kraut-Vass, A.; Allison, J. W.; Powell, C. J.; Rumble, J. R. NIST Standard Reference Database 20, version 3.4; web edition 2003.
- (14) Kitagawa, H.; Kojima, N.; Nakajima, T. *J. Chem. Soc., Dalton Trans.* **1991**, *11*, 3121.
- (15) Lieske, H.; Lietz, G.; Spindler, H.; Volter, J. *J. Catal.* **1983**, *81*, 8.
- (16) Lietz, G.; Lieske, H.; Spindler, H.; Hanke, W.; Volter, J. *J. Catal.* **1983**, *81*, 17.
- (17) Birgersson, H.; Eriksson, L.; Boutonnet, M.; Jaras, S. G. *Appl. Catal., B* **2004**, *54*, 193.
- (18) Galisteo, F. C.; Mariscal, R.; Granados, M. L.; Fierro, J. L. G.; Daley, R. A.; Anderson, J. A. *Appl. Catal., B* **2005**, *59*, 227.
- (19) Daley, R. A.; Christou, S. Y.; Efstathiou, A. M.; Anderson, J. A. *Appl. Catal., B* **2005**, *60*, 117.
- (20) Bernal, S.; Blanco, G.; Calvino, J. J.; Gatica, J. M.; Omil, J. A. P.; Pintado, J. M. *Top. Catal.* **2004**, *28*, 31.
- (21) Breen, J. P.; Burch, R.; Hardacre, C.; Hill, C. J.; Krutzsch, B.; Bandl-Konrad, B.; Jobson, E.; Cider, L.; Blakeman, P. G.; Peace, L. J.; Twigg, M. V.; Preise, M.; Gottschling, M. *Appl. Catal., B* **2007**, *70*, 36.
- (22) Romero-Sarria, F.; Martinez, L. M.; Centeno, M. A.; Odriozola, J. A. *J. Phys. Chem. C* **2007**, *111*, 14469.
- (23) Wootsch, A.; Descorme, C.; Duprez, D. *J. Catal.* **2004**, *225*, 259.
- (24) Comotti, M.; Della Pina, C.; Matarrese, R.; Rossi, M. *Angew. Chem., Int. Ed.* **2004**, *43*, 5812.
- (25) Pagliaro, M.; Ciriminna, R.; Kimura, H.; Rossi, M.; Della Pina, C. *Angew. Chem., Int. Ed.* **2007**, *46*, 4434.
- (26) Goguet, A.; Burch, R.; Chen, Y.; Hardacre, C.; Hu, P.; Joyner, R. W.; Meunier, F. C.; Mun, B. S.; Thompson, D.; Tibiletti, D. *J. Phys. Chem. C* **2007**, *111*, 16927.

JA9021705